


RESEARCH ARTICLE

Open Access



# Swd2/Cps35 determines H3K4 tri-methylation via interactions with Set1 and Rad6

Junsoo Oh<sup>1,2†</sup>, Shinae Park<sup>1,2†</sup>, Jueun Kim<sup>1,3</sup>, Soojin Yeom<sup>1,2</sup>, Ji Min Lee<sup>4</sup>, Eun-Jin Lee<sup>5\*</sup>, Yong-Joon Cho<sup>1,6\*</sup> and Jung-Shin Lee<sup>1,2\*</sup> 

## Abstract

**Background** Histone H3K4 tri-methylation (H3K4me3) catalyzed by Set1/COMPASS, is a prominent epigenetic mark found in promoter-proximal regions of actively transcribed genes. H3K4me3 relies on prior monoubiquitination at the histone H2B (H2Bub) by Rad6 and Bre1. Swd2/Cps35, a Set1/COMPASS component, has been proposed as a key player in facilitating H2Bub-dependent H3K4me3. However, a more comprehensive investigation regarding the relationship among Rad6, Swd2, and Set1 is required to further understand the mechanisms and functions of the H3K4 methylation.

**Results** We investigated the genome-wide occupancy patterns of Rad6, Swd2, and Set1 under various genetic conditions, aiming to clarify the roles of Set1 and Rad6 for occupancy of Swd2. Swd2 peaks appear on both the 5' region and 3' region of genes, which are overlapped with its tightly bound two complexes, Set1 and cleavage and polyadenylation factor (CPF), respectively. In the absence of Rad6/H2Bub, Set1 predominantly localized to the 5' region of genes, while Swd2 lost all the chromatin binding. However, in the absence of Set1, Swd2 occupancy near the 5' region was impaired and rather increased in the 3' region.

**Conclusions** This study highlights that the catalytic activity of Rad6 is essential for all the ways of Swd2's binding to the transcribed genes and Set1 redistributes the Swd2 to the 5' region for accomplishments of H3K4me3 in the genome-wide level.

**Keywords** H3K4 trimethylation, H2B ubiquitination, Rad6, Set1, Swd2

<sup>†</sup>Junsoo Oh and Shinae Park contributed equally to this work.

\*Correspondence:

Eun-Jin Lee  
eunjlee@korea.ac.kr  
Yong-Joon Cho  
yongjoon@kangwon.ac.kr  
Jung-Shin Lee  
jungshinlee@kangwon.ac.kr

<sup>1</sup> Department of Molecular Bioscience, College of Biomedical Science, Kangwon National University, Chuncheon 24341, Republic of Korea

<sup>2</sup> Institute of Life Sciences, Kangwon National University, Chuncheon 24341, Republic of Korea

<sup>3</sup> Kangwon Institute of Inclusive Technology, Kangwon National University, Chuncheon 24341, Republic of Korea

<sup>4</sup> Graduate School of Medical Science & Engineering, Korea Advanced Institute of Science and Technology, 291 Daehak-Ro, Yuseong-Gu, Daejeon 34141, Republic of Korea

<sup>5</sup> Department of Life Sciences, Korea University, Seoul 02841, Republic of Korea

<sup>6</sup> Multidimensional Genomics Research Center, Kangwon National University, Chuncheon 24341, Republic of Korea



## Background

Trimethylation of histone H3 lysine 4 (H3K4me3) is considered a hallmark of promoters of actively transcribed genes across diverse organisms from yeast to humans [1, 2]. Dysregulation of H3K4me3 and its modifiers has been linked to cancer pathogenesis and aberrant development in mammals, underscoring the importance of understanding its regulatory mechanisms [3–6]. The H3K4 methylation process, involving Set1/COMPASS methyltransferase, is highly conserved among eukaryotes, making budding yeast a valuable model for its study [1, 4]. Yeast Set1/COMPASS comprises Set1, an essential catalytic component, and seven accessory proteins, each contributing to protein stability or H3K4 methylating activity [7–10]. Swd2/Cps35 is the only essential component in Set1/COMPASS, because of its function within the cleavage and polyadenylation factor (CPF) transcription termination complex [9, 11, 12].

H3K4me3, as well as dimethylation, is dependent on monoubiquitination at the histone H2B (H2Bub) in yeast, fruit flies, and mammals [13–16]. A previous study has shown that Swd2/Cps35's binding to the rest of Set1/COMPASS is reduced in the absence of H2Bub and Swd2 addition to defective Set1/COMPASS, which was isolated from a strain deficient in H2Bub, enhances its *in vitro* H3K4me3 activity, emphasizing the importance of H2Bub-dependent binding of Swd2 to the rest of the Set1/COMPASS [17]. This previous study also showed that Swd2, rather than the rest of the Set1/COMPASS, was recruited by H2Bub into transcribed genes and facilitated the assembly of H3K4me3-competent Set1/COMPASS [17]. However, contrasting findings emerged by other groups: Rad6/H2Bub appeared necessary for Set1 and Swd2 occupancy on transcribed genes, with Set1 essential for Swd2 occupancy as well [11, 17]. These conflicting findings regarding Rad6/H2Bub's role in the occupancy of both Set1 and Swd2 on transcribed genes have raised questions, possibly due to variations in gene selection for chromatin immunoprecipitation (ChIP-qPCR) [11, 17].

In this study, we investigated the chromatin occupancy of Set1, Swd2, and Rad6 at the genome level. ChIP-seq data revealed that occupancy of the Swd2 appears on the transcribed genes with specific enrichments on both 5' region and 3' region of genes, which might be mediated through the tight interactions with Set1/COMPASS and CPF, respectively [7–9, 12]. Our results indicated that in the absence of the Rad6/H2Bub, Swd2 lost its occupancy through both ways on transcribed genes, but Set1 remains associated with the 5' region of transcribed genes. Intriguingly, in the absence of Set1, the peak of Swd2 on the 5' region was lost, but the peak on the 3' region rather increased, suggesting that Set1 and CPF are

competing with each other to obtain the common factor, Swd2, and Set1 is essential for redistributing Swd2 within transcribed genes, particularly to the 5' region.

This study expands the Rad6-dependent chromatin occupancy of Swd2 confirmed by ChIP-qPCR results in a previous study to the genome levels [17]. Also, more importantly, this study newly shows that occupancy of Swd2 to transcribed gene is majorly through Set1 or CPF, and both ways are dependent on Rad6's catalytic activity, and Set1 has a competitive relationship with CPF for Swd2. We believe that these data enhance the understanding of H2B ubiquitination-dependent H3K4me3 through Swd2/Cps35 and would be an important bridgehead to understand the relationship of two chromatin regulators (H2B ubiquitinase Rad6 and H3K4 methylase Set1) with transcriptional termination regulators (CPF).

## Results

### Determination of chromatin occupancy of Rad6, Swd2, and Set1 on transcribed genes

To improve our understanding of the correlation in transcribed gene occupancy between Rad6, Swd2, and Set1, we performed chromatin immunoprecipitation sequencing (ChIP-seq) for Rad6, Swd2, Set1, and H3K4me3. Epitope tags were added to the chromosomal copies of *RAD6* (Rad6-9Myc) or *SWD2* (Swd2-3HA) in yeast strains, and ChIP-seq was performed using antibodies against these tags. Additionally, ChIP-seq was performed with antibodies targeting Set1 and H3K4me3 in the wild-type strain. The distribution patterns of H3K4me3, Set1, Swd2, and Rad6 within the transcribed genes were obtained by sorting the yeast total genes ( $n = 6020$ ) based on their gene length (Fig. 1a).

To determine the localization of Rad6, Swd2, Set1, and H3K4me3 within a gene, we adopted a previously used gene classification method where total protein-coding genes in yeast into five groups depending on their length: extra-small, small, medium, large, and extra-large [18]. Based on the average distribution of H2Bub and H3K4me3 in the five gene groups, H2Bub was suggested to be evenly distributed along the gene while H3K4me3 was present in pronounced peaks in proximity to transcription start sites (TSS) regions [18]. Accordingly, we found that H2Bub ubiquitinase Rad6 was also evenly distributed along a gene while H3K4me3 was present as a sharp peak near the TSS regions (Fig. 1b, c). Similar to H3K4me3, Set1 and Swd2 peaks were found near the TSS regions (Fig. 1d, e). We analyzed the ChIP-exo data for H2B and H2Bub from GSE147927 through our pipelines (Additional file 1: Fig. S1a–e) [19]. Coincident with the localization of Rad6, the heatmaps and metagenes show that H2Bub was evenly distributed along a gene (Additional file 1: Fig. S1a–e). These typical distributions of

Rad6, Swd2, Set1, and H3K4me3 were also observed in integrative genomics viewer plots, highlighting the three representative genes (Fig. 1f).

To investigate the correlation between transcript levels and chromatin occupancy of Rad6, Swd2, Set1, and H3K4me3, we classified the total protein-coding genes in yeast ( $n=6020$ ) into high, medium, and low groups depending on the normalized transcript level of genes derived from mRNA-seq of the wild-type strain (data from GSE180992, [20]). As the transcript levels of genes increased, the chromatin occupancy of Rad6, Swd2, Set1, and H3K4me3 increased proportionally (Fig. 1g). Taken together, we confirmed that the transcription level of genes correlated with the chromatin occupancy of Rad6, Swd2, Set1, and H3K4me3. Furthermore, our results align with previous results, demonstrating that Rad6 and H2Bub are uniformly distributed along the gene [18]. In contrast, Set1 and Swd2 exhibited high occupancy in regions near the TSSs similarly to H3K4me3.

#### Significant levels of Set1 occupy the 5' region of transcribed genes in the absence of RAD6

To identify how Rad6 and Swd2 affect the Set1 occupancy on transcribed genes, we performed Set1 ChIP-seq in  $\Delta rad6$  and  $\Delta swd2$  strains. To remove the background signals of the Set1 ChIP-seq, we also performed ChIP-seq in the  $\Delta set1$  strain. Consequently, we confirmed that deleting *RAD6* reduced the occupancy of Set1 on transcribed genes at genome-wide levels, although enrichment was still observed near the 5' region of genes (Fig. 2a, c, d). To investigate whether reduction of Set1 occupancy in the  $\Delta rad6$  strain occurs with every yeast gene, we quantified the mapped reads per kilobase per million (RPKM) values of Set1 near the 5' region of genes ( $-100$  to  $+300$  bp of TSS) in both wild-type and  $\Delta rad6$  strains and displayed this as a scatter plot (Additional file 1: Fig. S2a). If Set1 occupancy near the 5' region of a gene in the  $\Delta rad6$  strain is similar to that of wild type, the dot is located near the  $y=x$  line (Additional file 1: Fig. S2a). Set1 occupancy at most genes was reduced in the  $\Delta rad6$  strain. Although

several genes retained similar Set1 occupancy in the wild-type strain, their length was too short to assess the Set1 occupancy compared with Set1 levels near the 5' region of genes. Therefore, Set1 occupancy is globally reduced at most *S. cerevisiae* genes in the  $\Delta rad6$  strain.

Although *SWD2* is an essential gene, the deletion strain of *SWD2* could be generated through overexpressing the truncated *SEN1* fragment [9]. Therefore, we performed Set1 ChIP-seq in Sen1-overexpressed wild-type (Sen1over WT) and  $\Delta swd2$  (Sen1over  $\Delta swd2$ ) strains. Subsequently, the occupancy of Set1 on transcribed genes disappeared in the  $\Delta swd2$  strain, which may have been caused by the severely reduced levels of Set1 protein [9] (Fig. 2a, b). Interestingly, we observed that the Set1 occupancy on transcribed genes in the Sen1over WT strain decreased to the same levels as that in the  $\Delta rad6$  strain, whereas the levels of Set1 protein and H3K4 di- and tri-methylation were similar to that of the wild-type strain (Fig. 2a–d). This western blot data agreed with the results of a previous study where the protein levels of Set1 were unaffected by overexpression of the *SEN1* fragment [9].

To identify how the occupancy of Set1 in the 5' region of genes is regulated by Sen1, we analyzed the Sen1 ChIP-exo data from GSE147927 (Additional file 1: Fig. S2b, c) [19]. In the heatmap, genes are sorted by gene length to more precisely confirm the localization of proteins on the transcribed genes (Additional file 1: Fig. S2b). The binding of Sen1 was detected across all transcribed genes with higher occupancy near the TSSs with a similar pattern to that of Set1, although the occupancy of Sen1 was closer to TSSs than that of Set1 (Additional file 1: Fig. S2b, c). Although how the overexpressed fragment of Sen1 interfered with the occupancy of Set1 on transcribed genes remained unclear, the occupancy levels of Set1 on transcribed genes in Sen1over WT strain was sufficient for significant cellular H3K4me3 and comparable with that of the  $\Delta rad6$  strain. These data suggest that in the absence of *RAD6*, Set1 occupancy is reduced to some extent but significant Set1 still occupies the 5' region of genes.

(See figure on next page.)

**Fig. 1** Determination of chromatin occupancy of Rad6, Swd2, and Set1 on transcribed genes. **a** The heatmaps represent the occupancy of H3K4me3, Set1, Swd2-3HA, and Rad6-9Myc in wild-type (WT) background around the TSS ( $\pm 1500$  bp) of total protein coding genes ( $n=6020$ ). **b–e** Yeast total protein-coding genes are classified into five groups depending on the gene length; XS ( $< 750$  bp), S ( $750 \sim 1500$  bp), M ( $1500 \sim 2250$  bp), L ( $2250 \sim 3000$  bp), and XL ( $3000 \sim 3750$  bp). The metagenome shows the average patterns of chromatin occupancy of **b** Rad6-9Myc, **c** H3K4me3, **d** Set1, and **e** Swd2-3HA. X-axis: 6000-bp window around the transcription start sites (TSSs); Y-axis: reads per million (RPM). **f** The IGV tracks show the enrichments of Rad6-9Myc, Swd2-3HA, Set1, and H3K4me3 at three representative genes, *YEF3*, *PYK1*, and *RP55*. **g** Yeast total protein-coding genes ( $n=6020$ ) are classified into three groups depending on reads per kilobase per million values of mRNA sequencing mapped to each gene. Number of genes of each group is 2006, 2006, and 2008 for high, medium, and low, respectively. Heatmaps show the occupancy of H3K4me3, Set1, Swd2-3HA, and Rad6-9Myc around the TSS ( $\pm 1500$  bp) of highly transcribed genes (high), medium transcribed genes (medium), and lowly transcribed genes (low)

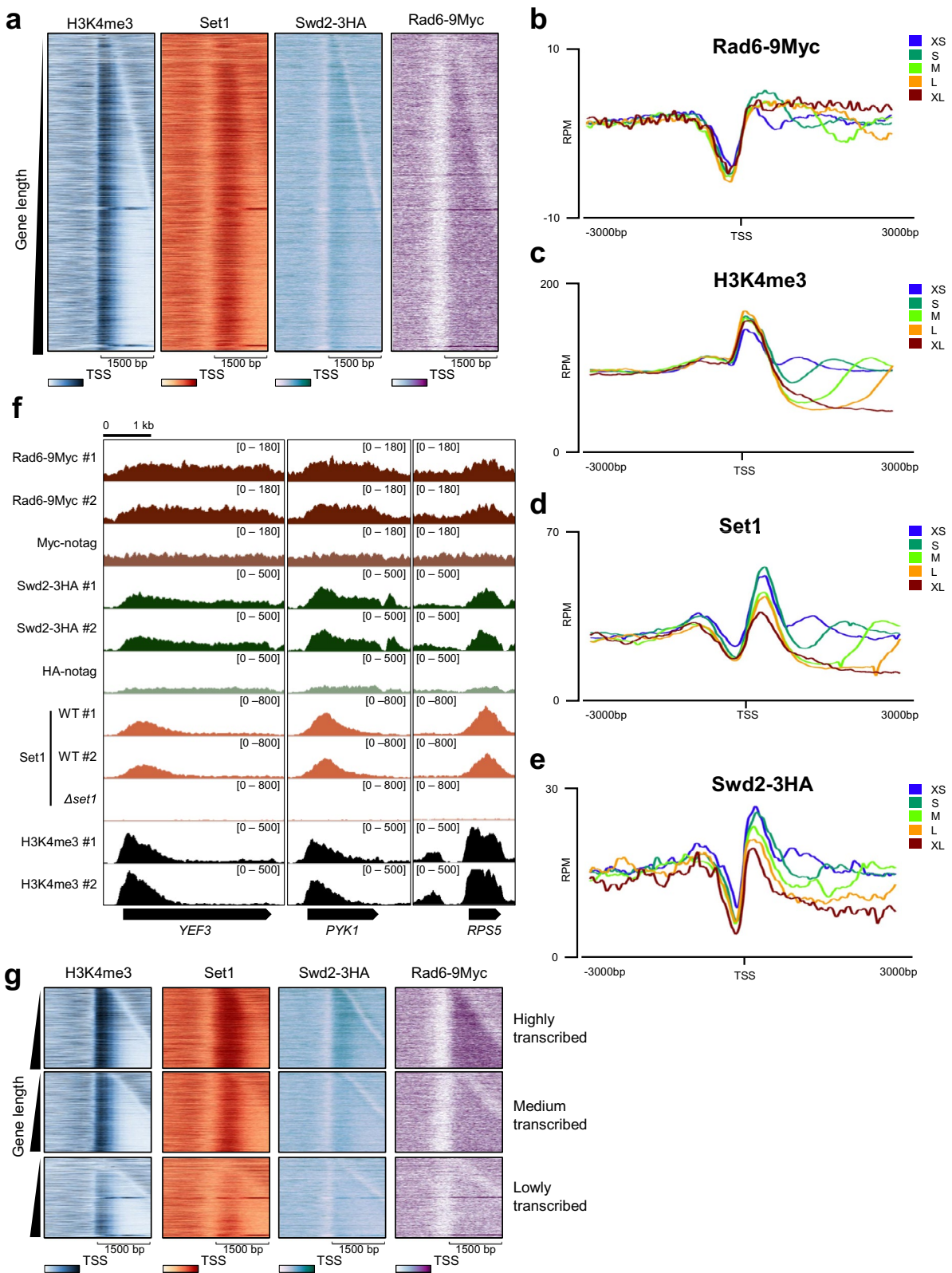


**Fig. 1** (See legend on previous page.)



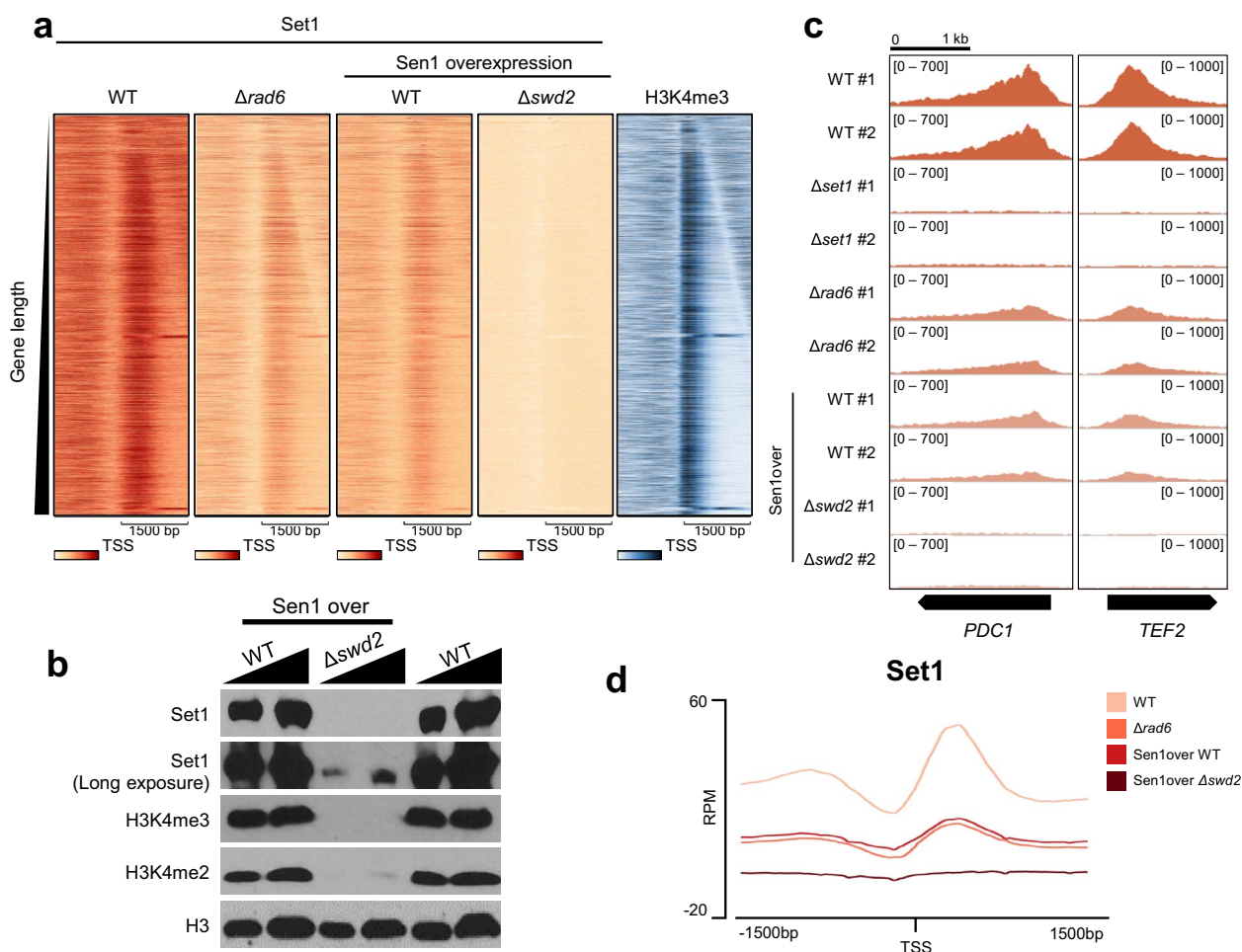


**Fig. 2** Significant Set1 occupies the 5' region of transcribed genes in the absence of *RAD6*. **a** The heatmaps represent the occupancy of Set1 in wild-type (WT),  $\Delta rad6$ , Sen1 over WT, and Sen1 over  $\Delta swd2$ , and H3K4me3 of wild-type strain around the TSS ( $\pm 1500$  bp) of total protein coding genes ( $n = 6020$ ). **b** The levels of Set1, H3K4me3, H3K4me2, and H3 in the Sen1 over WT, Sen1 over  $\Delta swd2$ , and wild-type strains were measured by western blotting. **c** The IGV tracks show the enrichments of Set1 at two representative genes, *PDC1* and *TEF2*, in WT,  $\Delta set1$ ,  $\Delta rad6$ , Sen1 over WT and Sen1 over  $\Delta swd2$  strains. **d** The metagenes represent the average distribution of Set1 near TSS regions ( $\pm 1500$  bp) of total protein-coding genes ( $n = 6020$ ) in WT,  $\Delta rad6$ , Sen1 over WT, and Sen1 over  $\Delta swd2$  strains

### Catalytic activity of Rad6 is essential for the occupancy of Swd2 on transcribed genes

To identify H2Bub-dependent chromatin occupancy of Swd2 at the genome-wide level, we added a 3HA tag to a chromosomal copy of *SWD2* in wild-type or  $\Delta rad6$  background strains and conducted ChIP-seq with an anti-HA antibody (Fig. 3a–c); we also performed ChIP-seq in the untagged strain to remove the background signals of the HA tag ChIP-seq. We sorted the total protein-coding genes in yeast by gene length and compared the binding pattern with that of H3K4me3 (Fig. 3a). In the  $\Delta rad6$  strain, although the protein level of Swd2-3HA was not decreased, the occupancy of Swd2 on transcribed genes was significantly reduced at most protein-coding genes (Fig. 3a–d). The reduced chromatin binding of Swd2 in the  $\Delta rad6$  strain was

comparable with that of the background signals in the untagged strain, indicating the removal of Swd2 binding upon *RAD6* deletion (Fig. 3a–c).

To identify whether the catalytic activity of Rad6 is important for the occupancy of Swd2 on transcribed genes, we chromosomally tagged Swd2 (*SWD2-3HA*) in the Rad6-9Myc wild-type and catalytically inactive Rad6-C88A-9Myc strains (Fig. 3e). Although H2Bub and H3K4me3 disappeared, the protein levels of Swd2-3HA remained unchanged in the Rad6-C88A strain (Fig. 3e). We compared the Swd2-3HA ChIP-seq in the Rad6-C88A strain with that of isogenic wild-type strain, and the results show that the occupancy of Swd2 on transcribed genes was severely reduced in the Rad6 catalytic dead mutant (Fig. 3f).

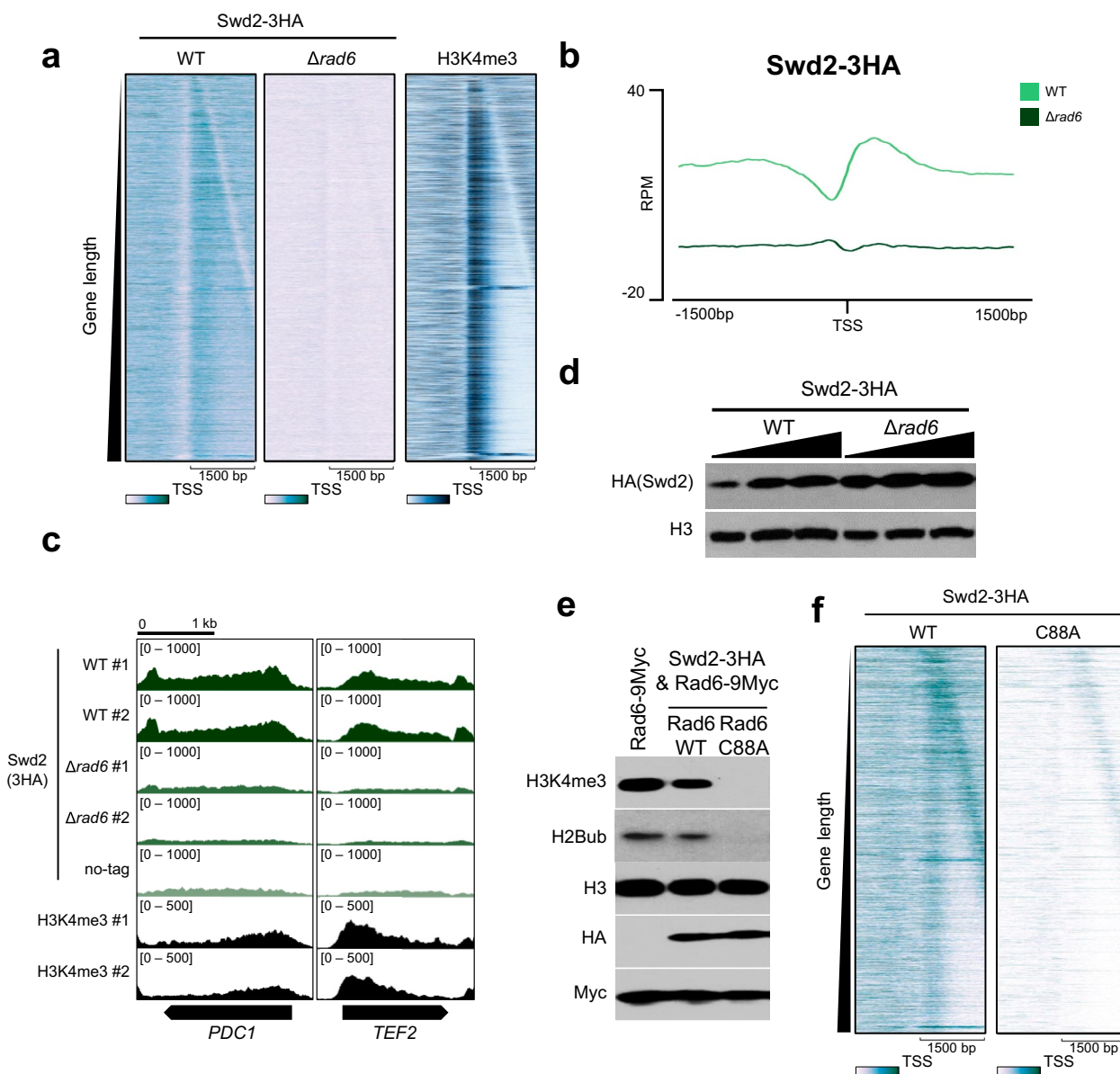


**Fig. 3** Catalytic activity of Rad6 is essential for the occupancy of Swd2 on transcribed genes. **a** The heatmaps represent the occupancy of Swd2-3HA in wild-type (WT) or  $\Delta rad6$  background and H3K4me3 around the TSS ( $\pm 1500$  bp) of total protein coding genes ( $n = 6020$ ). **b** The metagenes represent the average distribution of Swd2-3HA near TSS regions ( $\pm 1500$  bp) of total protein coding genes ( $n = 6020$ ) of WT and  $\Delta rad6$  strains. **c** The IGV tracks show the Swd2-3HA enrichments in WT or  $\Delta rad6$  background and H3K4me3 at two representative genes, *PDC1* and *TEF2*. **d** The protein levels of Swd2-3HA in *SWD2-3HA* WT and *SWD2-3HA*  $\Delta rad6$  were measured by western blotting. **e** The levels of H3K4me3, H2Bub, H3, Myc (Rad6-9Myc), and HA (Swd2-3HA) in the Rad6-9Myc WT, Swd2-3HA and Rad6-9Myc, and Swd2-3HA and Rad6-C88A-9Myc strains were measured by western blotting. **f** The heatmaps represent the occupancy of Swd2-3HA in wild-type (WT) or Rad6-C88A background around the TSSs ( $\pm 1500$  bp) of total protein-coding genes ( $n = 6020$ )

The levels of H2Bub and H3K4me3 were reduced by the addition of the 3HA tag at the C-terminus of *SWD2* (*SWD2-3HA*), and epitope tagging of Swd2 would therefore induce defects in the function of Swd2 to some extents (Fig. 3e). Nevertheless, considering that significant amount of H2Bub and H3K4me3 still remained, and the catalytic dead mutant of Rad6 still

possesses the 3HA tagged Swd2, we consider that the impairment of Swd2 binding in the Rad6-C88A mutant results from the loss of the Rad6’s catalytic activity. Overall, the transcribed gene occupancy of Swd2 was completely dependent on Rad6 and its catalytic activity at most protein-coding genes. However, a significant amount of Set1 proteins could already occupy

transcribed genes in the absence of Rad6, though this occupancy was enhanced by Rad6.

### Set1 redistributes Swd2 within transcribed genes to the 5' region

To identify whether Set1 is required for Swd2 occupancy, we performed HA ChIP-seq in yeast strains containing chromosomal *SWD2-6HA* in the wild-type and  $\Delta set1$  backgrounds. The protein levels of Swd2-6HA were unchanged by the deletion of *SET1* (Fig. 4a). The heatmaps show that peaks of Swd2 near TSSs were uniformly located from TSSs independently of the gene length in the wild-type condition (Fig. 4b). By contrast, in the  $\Delta set1$  strain, the Swd2 peaks near the TSSs decreased, but the occupancy of Swd2 increased at both of the other regions within transcribed genes and specifically at the transcription termination sites (TTSs) (Fig. 4b, c). In addition to being a component of Set1/COMPASS, Swd2 is a component of CPF transcription termination factors [36, 37]. Therefore, we also examined the occupancy of Swd2 near TTSs (Fig. 4c). To identify whether the occupancy of Swd2 in  $\Delta set1$  strain was similar to that of CPF complex components, we analyzed the ChIP-exo data of three components of CPF, Cft1, Pap1, and Ref2 from GSE147927 (Fig. 4d, e) [19]. The heatmaps illustrated that the global localization of Swd2 in the  $\Delta set1$  strain was similar to the occupancy of the three components of CPF (Fig. 4e and Additional file 1: Fig. S3). Notably, the occupancy of both Swd2 in the  $\Delta set1$  strain and the CPF occurred across the transcribed genes as well as near the TTSs. However, the occupancy of Swd2 across the transcribed genes and near the TTSs in both the  $\Delta rad6$  and Rad6-C88A strains disappeared (Fig. 4f, g).

### Discussion

H3K4me3 serves as a well-established hallmark indicative of active transcription, and numerous studies have elucidated the underlying molecular mechanisms associated with it. In the context of mammals, H3K4me3 plays a pivotal role in cell differentiation and development processes [4, 5]. In the case of differentiated cells, the H3K4me3 domain at the promoters of lineage

determination factors is required to maintain cell identity [21]. A recent research endeavor has shed light on the involvement of H3K4me3 in global transcription regulation through RNA polymerase II pause-release [6]. Furthermore, it is well-documented that H3K4me3 is dependent on H2Bub in various organisms including yeast, fruit flies, and mammals [13, 14, 16, 22]. Therefore, unraveling the mechanistic interplay between H2Bub and H3K4me3 via Set1/COMPASS is of paramount importance in comprehending the evolutionary conservation of H3K4me3 [13, 14, 22, 23].

Summary of this study is highlighted in Fig. 5. Swd2/Cps35 and its orthologs in *Drosophila* and mammals are required for the H2Bub-dependent H3K4me3 [17, 22, 23]. So, how the Swd2/Cps35 occupies the 5' region of genes for H3K4me3 is an important issue for understanding the H2Bub-dependent H3K4me3. We reveal that two major Swd2 peaks exist near the 5' region and 3' region of genes. This study posits that Swd2 can establish its presence on transcribed genes through at least two mechanisms: (1) via the Set1/COMPASS and (2) through association with the CPF. It is noteworthy that the two pathways, owing to their close association with Swd2, are likely the most predominant pathways [7, 8, 12]. Our data support that catalytic activity of Rad6 is essential for all the peaks of Swd2 on the transcribed genes, that is, not only for the occupancy of Swd2 near the 5' region, but also required for the Swd2 near the 3' region. Based on the Swd2-6HA ChIP-seq data in the absence of the *SET1*, we realized that Set1 redistributes Swd2 to the 5' region for accomplishments of its H3K4me3. Interestingly, the data suggest that Set1 competes with CPF to obtain quantitatively limited Swd2. Taken together, this study reveals that Rad6/H2Bub is essential for the occupancy of Swd2 on most genes in yeast, and Set1 redistributes Swd2 to the 5' region of genes for H3K4me3 in the regions. Also, the results that catalytic activity of Rad6 is also required for the Swd2's occupancy on the 3' region and Set1 competes with CPF for Swd2 shed light on the potential regulation of CPF by Rad6 (or H2Bub) and Set1 (or H3K4me) through Swd2.

(See figure on next page.)

**Fig. 4** Set1 redistributes Swd2 within transcribed genes to the 5' region. **a** The protein levels of Swd2-6HA in *SWD2-6HA* WT, *SWD2-6HA*  $\Delta set1$ , and WT (notag) were measured by western blotting. The heatmaps show the occupancy of Swd2-6HA at 3000-bp window near **b** the transcription start sites (TSSs) or **c** the transcription termination sites (TTSs) in WT or  $\Delta set1$  condition. **d** The IGV tracks show the enrichments of Swd2-6HA in WT or  $\Delta set1$  background, and the three components of CPF, Cft1, Pap1, and Ref2 at three representative genes, *PMA1*, *PYK1*, and *YEF3*. The ChIP-exo data of Cft1, Pap1, and Ref2 have been obtained from GSE147927 and processed by our pipeline. **e** The heatmaps show the occupancy of Swd2-6HA in  $\Delta set1$  strain, and three components of CPF, Cft1, Pap1, and Ref2 in wild-type strain around the transcription termination sites ( $\pm 1500$  bp of TTSs). **f** The heatmaps represent the occupancy of Swd2-3HA in WT or  $\Delta rad6$  background around the transcription termination site ( $\pm 1500$  bp of TTSs) of total protein-coding genes ( $n=6020$ ). **g** The heatmaps represent the occupancy of Swd2-3HA in WT or Rad6-C88A background around the TTSs ( $\pm 1500$  bp) of total protein-coding genes ( $n=6020$ )



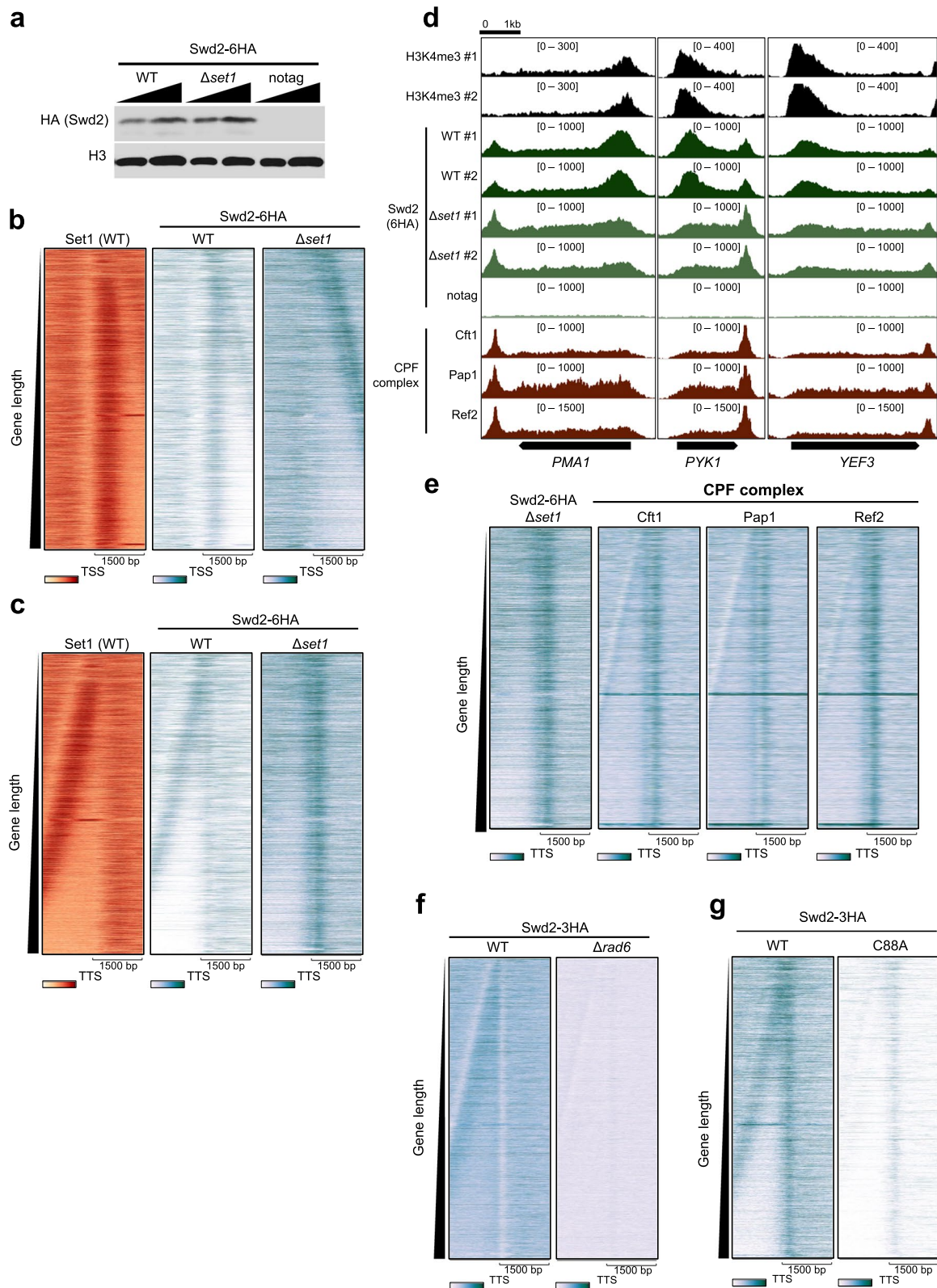
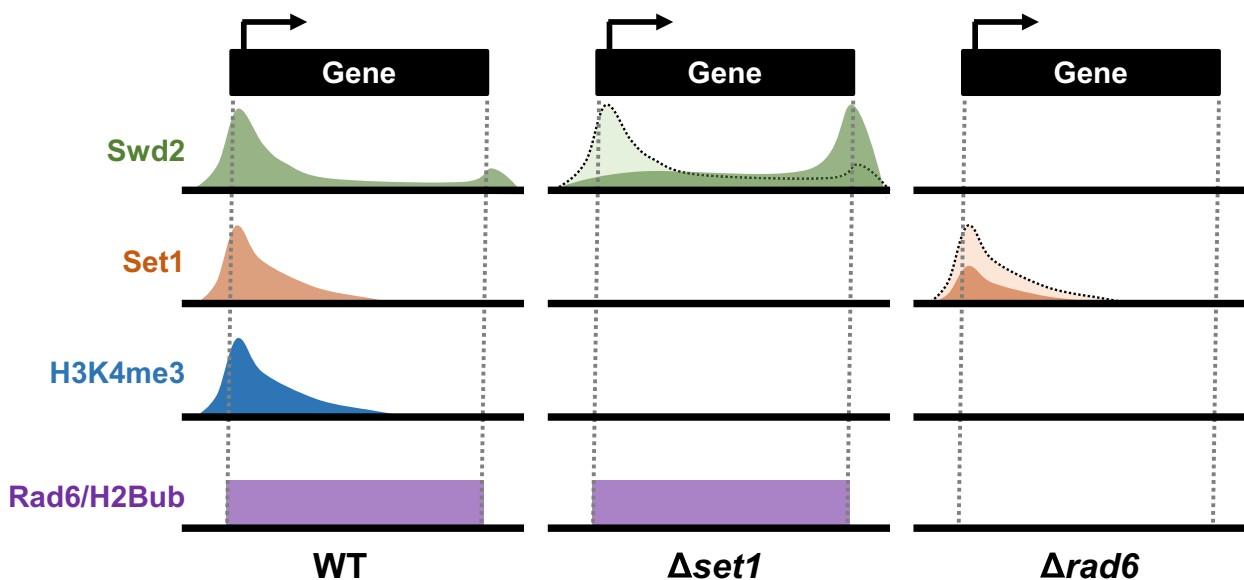


**Fig. 4** (See legend on previous page.)





\*Localization of Swd2 in  $\Delta set1$  is almost same to that of the CPF components (Ref2, Cft1, Pap1)

**Fig. 5** Summary: occupancy of Swd2 on transcribed genes is differentially regulated by Set1 and Rad6

An interesting finding is that H2Bub by Rad6 would give authority to Set1 to lead the Swd2's positioning to the 5' region of genes. In the presence of H2Bub/Rad6, Set1 redistributes Swd2 to the 5' region of genes (Fig. 4). However, in the absence of H2Bub/Rad6, while significant Set1 occupies the 5' region of genes, these Set1 proteins did not contribute to the 5' region positioning of Swd2 at all (Figs. 2 and 3). These data suggest that the Swd2 functions as a mediator translating the signal of H2Bub by Rad6 to the COMPASS. Two previous studies revealed the Swd2's roles to mediate the H2Bub-dependent H3K4me3 [17, 24]. A study observed the loss of Swd2 from chromatin and the COMPASS purified from the H2Bub-deficient strains [17]. The other study revealed the H2Bub-dependent ubiquitination of Swd2, which is crucial for the H3K4me3 [24]. Based on these findings, a plausible model explaining how H2Bub promotes the Set1-dependent positioning of Swd2 to the 5' region is that the binding of Swd2 to Set1 is enhanced, although the exact mechanisms remain to be identified. The direct modifications of Swd2 or other Set1 complexes and the involvement of the 3rd factor dependent on H2Bub would be the potential candidates.

Our data also unveil that Swd2 occupancy on the 3' region of transcribed genes depends on the catalytic activity of Rad6 and is inhibited by Set1. An interesting finding is that both Set1 and Rad6 are required for the occupancy of Swd2 on the 5' region but have the contrary roles for the occupancy on the 3' region

(Figs. 3 and 4). CPF-dependent Swd2 occupancy on the 3' region is also dependent on H2Bub by Rad6, albeit further studies are warranted to ascertain whether the Rad6-mediated impact extends to the association of Swd2 with the CPF complex. Also, whether and how the H2Bub and H3K4 methylation affect the transcription termination by CPF through Swd2/Cps35 component should be identified through further studies. We believe that the data in this manuscript could be a bridgehead for studies regarding the relationship between a promoter-proximally positioned H3K4me3 and transcription termination by CPF.

Swd2 is an essential protein, although the deletion strain is viable in specific conditions. Interestingly, the lethality associated with *SWD2* can be suppressed by three distinct interventions: the deletion of *SET1* or *RAD6* and the overexpression of the *SEN1* fragment [9, 11]. A prior study hinted at the presence of an antagonistic relationship between the Set1/COMPASS and the CPF complex, both of which share an essential component Swd2 [11]. This study provided evidence that the three aforementioned conditions collectively attenuate the occupancy of Set1 upon transcribed genes. However, it remains an open question whether the reduced Set1 occupancy under these conditions serves as a common underlying mechanism for mitigating the lethality associated with *SWD2* deletion. Further research is needed to establish this causative link definitively.

## Conclusions

Our study revealed that two major Swd2 peaks exist near the 5' region by Set1 and the 3' region of genes which might be through the CPF. Our data support that the catalytic activity of Rad6 is essential for occupancy of Swd2 through both modes, and Set1 is required for the redistribution of Swd2 from the 3' region to 5' region, suggesting the competition between COMPASS and CPF for Swd2. This study is a bridgehead for the detailed understanding of H2Bub-dependent H3K4me3 and the potential functional relationship between H3K4 methylation by Set1 and transcription termination by CPF through its common factor Swd2/Cps35.

## Methods

### Strains

Strains used in this study are presented in Additional file 5: Table S1.

### Antibodies

The following antibodies were used in this study for the western blot and the ChIP assay: anti-H3K4me3 (Millipore Cat# 07-473, RRID: AB\_1977252; 1/50,000 dilution for WB; 1  $\mu$ l was added to a chromatin extract for ChIP), anti-H2Bub1 (Cell Signaling Technology Cat# 5546, RRID:AB\_10693452; 1/2500 dilution for WB), anti-c-Myc (9E10) (Santa Cruz Biotechnology Cat# sc-40, RRID:AB\_627268; 1/5000 dilution for WB; 10  $\mu$ l was added to a chromatin extract for ChIP), and anti-HA (Santa Cruz Biotechnology Cat# sc-7392, RRID:AB\_627809; 1/5000 dilution for WB; 2.5  $\mu$ l was added to a chromatin extract for ChIP). Anti-H3 (1/100,000 dilution for WB), anti-H3K4me2 (1/50,000 dilution for WB), and anti-Set1 (1/5000 dilution for WB; 2.5  $\mu$ l was added to a chromatin extract for ChIP) were obtained from Shilatifard's laboratory [15, 17].

### Western blot (WB)

Cell extract was prepared from overnight cultured cells in YPD (YP-dextrose) media at 30 °C. Harvested cells were homogenized by vortexing at 4 °C for 30 min. The lysates were boiled with loading dye and then analyzed for western blotting. Proceeding steps were performed as a previous study [17]. The western data in the main figures are the representative data of biologically duplicated results.

### Chromatin immunoprecipitation (ChIP)

ChIP assays were performed as described previously [17]. Briefly, cells were grown to the exponential phase (OD<sub>600</sub> of 1.0) at 30 °C and harvested after cross-linking with formaldehyde for 5 min and quenching with

2.5 M glycine for 20 min. Cells were resuspended with FA-lysis buffer, and 0.5-mm glass beads were added. Bead beating was performed for 30 min at 4 °C, and the chromatin of lysed cells was sheared by sonication. Immunoprecipitation was performed with antibodies against Rad6-9Myc, Swd2-3HA, Swd2-6HA, Set1, and H3K4me3. In Rad6-9Myc, Swd2-3HA, Swd2-6HA, Set1, and H3K4me3 for ChIP experiments, 5% of chromatin extract of *Candida albicans*  $\Delta$ set1 strain (set1 null mutant ( $\Delta$ SETdU) from [25]; for Set1 ChIP-seq) or 10% of chromatin extract of *Schizosaccharomyces pombe* (strain 972 h- (ATCC 24843); for the other ChIP-seqs) was added for spike-in normalization. The A/G agarose (#sc-2003, Santa Cruz Biotechnology) was used for precipitating the DNA. After washing, reverse cross-linking and DNA precipitation were performed.

### ChIP-seq and analysis

ChIP-seq DNA samples were quantified by QuantiT PicoGreen dsDNA Assay kit, and 10 ng of DNA was used for the starting material of library preparation. ChIP-Seq library was constructed with NEBNext<sup>®</sup> ChIP-Seq Library Prep Master Mix Set for Illumina<sup>®</sup> (#E6240, NEB) according to the manufacturer's instructions. Sequencing was performed using Illumina HiSeq 2500 System (RRID:SCR\_016383) by the manufacturer's protocol, and 51-bp single-end reads were generated for each sample. The sequencing adapter removal and quality-based trimming were performed by Trimmomatic v.0.36 (RRID:SCR\_011848) [26]. Cleaned reads were mapped to the reference genome using Bowtie 2 (RRID:SCR\_016368) v.2.2.5 with the default parameter [27]. *S. pombe* reads were calculated and used for normalization by adjusting spike-in reads to one million reads for each sample. The resulted data were used for visualization by EaSeq [28] and Integrative Genomics Viewer (IGV) (RRID:SCR\_011793) [29].

ChIP-seq for Rad6-9Myc, Swd2-3HA (WT,  $\Delta$ rad6 or Rad6-C88A), Swd2-6HA (WT or  $\Delta$ set1), Set1 (WT,  $\Delta$ set1,  $\Delta$ rad6, Sen1over WT, or Sen1over  $\Delta$ swd2), and H3K4me3 were performed in biologically duplicate. We performed ChIP-seq using Myc or HA antibodies with a strain without any epitope tag (No-tag) once to consider the background signals by non-specific binding. IGV track data in this manuscript were drawn with the resulting data. Then, the Myc or HA signals to the No-tag control strain were subtracted from each of the duplicate ChIP-seq data of Myc-tagged Rad6 (Rad6-9Myc) or HA-tagged Swd2 (Swd2-3HA or Swd2-6HA), respectively. Data supporting the reproducibility of the resulting duplicate ChIP-seq data were included in this paper with the Additional file2 (Data supporting the reproducibility of the ChIP-seq results). The average values of the

duplicate data were used for the heatmaps and metagene plots in this manuscript.

Total protein-coding genes ( $n=6020$ ) were selected after excluding noncoding exons from 7589 genes of the *sacCer3* reference genome (Uniprot, 07/15/2017 version). After calculating the mean RPM (reads per million) values of each gene, heatmaps and anchor plots were drawn through the guidance of EaSeq [28].

#### Abbreviations

H3K4me3	Histone H3K4 tri-methylation
H2Bub	Histone H2B K123 mono-ubiquitination
COMPASS	Complex of proteins associated with Set1
CPF	Cleavage and polyadenylation factor
ChIP	Chromatin immunoprecipitation
qPCR	Quantitative PCR
ChIP-seq	Chromatin immunoprecipitation sequencing
TSS	Transcription start site
RPKM	Reads per kilobase per million
HA	Hemagglutinin
TTS	Transcription termination site

#### Supplementary Information

The online version contains supplementary material available at <https://doi.org/10.1186/s12915-024-01903-3>.

**Additional file 1: Fig. S1.** Determination of H2B ubiquitination on transcribed gene. **a** The heatmaps represent the occupancy of H2B and H2BK123 ubiquitination around the TSSs (Transcription start sites;  $\pm 1500$ bp) of total protein coding genes ( $n = 6020$ ). **b-e** Metagenes show the average distribution of **b-c** H2B or **d-e** H2Bub around the TSS ( $\pm 1,500$ bp) in WT strain. **Fig. S2.** Significant levels of Set1 occupy the 5' region of transcribed genes in the absence of *RAD6*. **a** The scatter plot represents the normalized Set1 occupancy near TSSs (from -100bps to +300bps of TSSs) of total protein coding genes ( $n = 6020$ ) in WT and  $\Delta rad6$  strains. To calculate the normalized Set1 occupancy near TSSs, after the RPKM values of Set1 ChIP-seq mapped near TSSs (from -100bps to +300bps of TSSs) in WT,  $\Delta rad6$  and  $\Delta set1$  strains had been calculated, the values of  $\Delta set1$  strains have been subtracted from the Wildtype and  $\Delta rad6$  strains. **b** The heatmaps represent the occupancy of Sen1 and Set1 around the TSSs (Transcription start sites;  $\pm 1500$ bp) of total protein coding genes ( $n = 6,020$ ). **c** The IGV tracks show the enrichments of Sen1 in WT strain, and Set1 in WT,  $\Delta set1$  and Sen1 over WT strains at three representative genes, *PMA1*, *PYK1* and *YEF3*. **Fig. S3.** Set1 redistributes Swd2 within transcribed genes to the 5' region. The heatmaps show the occupancy of Swd2-6HA in  $\Delta set1$  strain, and three CPF complex components, Cft1, Pap1 and Ref2 in wildtype strain around the transcription start sites ( $\pm 1500$ bp of TSSs).

**Additional file 2.** Data supporting the reproducibility of the ChIP-seq results.

**Additional file 3.** Uncropped blots for western blot data.

**Additional file 4.** Reads of spikes-in chromatin mapped to the genome of *C. albicans* (for Set1 ChIP-seq) or *S. pombe* (other ChIP-seqs).

**Additional file 5: Table S1.** Strains used in this study.

#### Acknowledgements

We thank Ali Shilatifard for providing the antibodies and strains for the chromatin occupancy of Swd2 and Rad6.

#### Authors' contributions

JL1 designed the research. YC, JO, and SP performed the bioinformatics analysis. JO and SP analyzed the data and performed the research. JL1, JO, and SP wrote the paper. JL1, JO, SP, YC, EL, JL2, JK, and SY revised the paper. All authors read and approved the final manuscript.

#### Funding

This work was supported by the National Research Foundation of Korea grants funded by the Korean government (Ministry of Science and ICT) (NRF-2020R111A3072234, NRF-2023R1A2C1003170, and RS-2023-00260267 to J.L.; NRF-2021R1C1C2005724 to S.P.), the Ministry of Education (NRF-2020R1A6A3A13077356 and NRF-2022R1A6A3A01087657 to J.O., RS-2023-00250980 to J.K., and RS-2023-00274760 to S.Y.), and the LAMP program through the National Research Foundation of Korea funded by the Ministry of Education (RS-2023-00301850 to Y.C.).

#### Availability of data and materials

All data generated or analyzed during this study are included in this published article and its supplementary information files (Additional files 1, 2, 3 and 4) and publicly available repositories. The yeast strains generated in this study are included in Additional file 5 and available from the corresponding authors upon request.

Sequencing datasets are available in the NCBI Gene Expression Omnibus (GEO; <https://www.ncbi.nlm.nih.gov/geo/>). Swd2-3HA(WT,  $\Delta rad6$ , Rad6-C88A), Rad6-9Myc (WT, Rad6-C88A), and Swd2-6HA(WT,  $\Delta set1$ ) ChIP-seq datasets: accession number GSE193209 (<https://www.ncbi.nlm.nih.gov/geo/query/acc.cgi?acc=GSE193209>). Set1 ChIP-seq datasets in WT,  $\Delta set1$ ,  $\Delta rad6$ , Sen1 overexpressed WT, and  $\Delta swd2$  strains: accession number GSE234564 (<https://www.ncbi.nlm.nih.gov/geo/query/acc.cgi?acc=GSE234564>). H3K4me3 ChIP-seq datasets containing the wild-type strain: GSE261160 (<https://www.ncbi.nlm.nih.gov/geo/query/acc.cgi?acc=GSE261160>). ChIP-exo data for H2B, H2Bub, Sen1, Cft1, Pap1, and Ref2 from GSE147927 (<https://www.ncbi.nlm.nih.gov/geo/query/acc.cgi?acc=GSE147927>) [19]. mRNA-seq data of the wild-type strain from GSE180992 (<https://www.ncbi.nlm.nih.gov/geo/query/acc.cgi?acc=GSE180992>) [20].

#### Declarations

##### Ethics approval and consent to participate

Not applicable.

##### Consent for publication

Not applicable.

##### Competing interests

The authors declare that they have no competing interests.

Received: 19 September 2023 Accepted: 24 April 2024

Published online: 03 May 2024

#### References

- Howe FS, Fischl H, Murray SC, Mellor J. Is H3K4me3 instructive for transcription activation? *BioEssays*. 2017;39(1):1–12.
- Santos-Rosa H, Schneider R, Bannister AJ, Sherriff J, Bernstein BE, Emre NC, Schreiber SL, Mellor J, Kouzarides T. Active genes are tri-methylated at K4 of histone H3. *Nature*. 2002;419(6905):407–11.
- Park S, Kim GW, Kwon SH, Lee JS. Broad domains of histone H3 lysine 4 trimethylation in transcriptional regulation and disease. *FEBS J*. 2020;287(14):2891–902.
- Shilatifard A. The COMPASS family of histone H3K4 methylases: mechanisms of regulation in development and disease pathogenesis. *Annu Rev Biochem*. 2012;81:65–95.
- Cenik BK, Shilatifard A. COMPASS and SWI/SNF complexes in development and disease. *Nat Rev Genet*. 2021;22(1):38–58.
- Wang H, Fan Z, Shliha PV, Miele M, Hendrickson RC, Jiang X, Helin K. H3K4me3 regulates RNA polymerase II promoter-proximal pause-release. *Nature*. 2023;615(7951):339–48.
- Miller T, Krogan NJ, Dover J, Erdjument-Bromage H, Tempst P, Johnston M, Greenblatt JF, Shilatifard A. COMPASS: a complex of proteins associated with a trithorax-related SET domain protein. *Proc Natl Acad Sci U S A*. 2001;98(23):12902–7.

8. Roguev A, Schaft D, Shevchenko A, Pijnappel WW, Wilm M, Aasland R, Stewart AF. The *Saccharomyces cerevisiae* Set1 complex includes an Ash2 homologue and methylates histone 3 lysine 4. *EMBO J*. 2001;20(24):7137–48.
9. Nedeá E, Nalbant D, Xia D, Theoharis NT, Suter B, Richardson CJ, Tatchell K, Kislinger T, Greenblatt JF, Nagy PL. The Glc7 phosphatase subunit of the cleavage and polyadenylation factor is essential for transcription termination on snoRNA genes. *Mol Cell*. 2008;29(5):577–87.
10. Mersman DP, Du HN, Fingerma IM, South PF, Briggs SD. Charge-based interaction conserved within histone H3 lysine 4 (H3K4) methyltransferase complexes is needed for protein stability, histone methylation, and gene expression. *J Biol Chem*. 2012;287(4):2652–65.
11. Soares LM, Buratowski S. Yeast Swd2 is essential because of antagonism between Set1 histone methyltransferase complex and APT (associated with Pta1) termination factor. *J Biol Chem*. 2012;287(19):15219–31.
12. Casanal A, Kumar A, Hill CH, Easter AD, Emsley P, Degliesposti G, Gordiyenko Y, Santhanam B, Wolf J, Wiederhold K, et al. Architecture of eukaryotic mRNA 3'-end processing machinery. *Science*. 2017;358(6366):1056–9.
13. Dover J, Schneider J, Tawiah-Boateng MA, Wood A, Dean K, Johnston M, Shilatifard A. Methylation of histone H3 by COMPASS requires ubiquitination of histone H2B by Rad6. *J Biol Chem*. 2002;277(32):28368–71.
14. Sun ZW, Allis CD. Ubiquitination of histone H2B regulates H3 methylation and gene silencing in yeast. *Nature*. 2002;418(6893):104–8.
15. Schneider J, Wood A, Lee JS, Schuster R, Dueker J, Maguire C, Swanson SK, Florens L, Washburn MP, Shilatifard A. Molecular regulation of histone H3 trimethylation by COMPASS and the regulation of gene expression. *Mol Cell*. 2005;19(6):849–56.
16. Kim J, Guermah M, McGinty RK, Lee JS, Tang Z, Milne TA, Shilatifard A, Muir TW, Roeder RG. RAD6-mediated transcription-coupled H2B ubiquitylation directly stimulates H3K4 methylation in human cells. *Cell*. 2009;137(3):459–71.
17. Lee JS, Shukla A, Schneider J, Swanson SK, Washburn MP, Florens L, Bhau-mik SR, Shilatifard A. Histone crosstalk between H2B monoubiquitination and H3 methylation mediated by COMPASS. *Cell*. 2007;131(6):1084–96.
18. Schulze JM, Hentrich T, Nakanishi S, Gupta A, Emberly E, Shilatifard A, Kobor MS. Splitting the task: Ubp8 and Ubp10 deubiquitinate different cellular pools of H2BK123. *Genes Dev*. 2011;25(21):2242–7.
19. Rossi MJ, Kuntala PK, Lai WKM, Yamada N, Badjatia N, Mittal C, Kuzu G, Bocklund K, Farrell NP, Blanda TR, et al. A high-resolution protein architecture of the budding yeast genome. *Nature*. 2021;592(7853):309–14.
20. Oh J, Kim S, Kim S, Kim J, Yeom S, Lee JS. An epitope-tagged Swd2 reveals the different requirements of Swd2 concentration in H3K4 methylation and viability. *Biochim Biophys Acta Gene Regul Mech*. 2024;1867(2):195009.
21. Benayoun BA, Pollina EA, Ucar D, Mahmoudi S, Karra K, Wong ED, Devarajan K, Daugherty AC, Kundaje AB, Mancini E, et al. H3K4me3 breadth is linked to cell identity and transcriptional consistency. *Cell*. 2014;158(3):673–88.
22. Mohan M, Herz HM, Smith ER, Zhang Y, Jackson J, Washburn MP, Florens L, Eissenberg JC, Shilatifard A. The COMPASS family of H3K4 methylases in *Drosophila*. *Mol Cell Biol*. 2011;31(21):4310–8.
23. Wu M, Wang PF, Lee JS, Martin-Brown S, Florens L, Washburn M, Shilatifard A. Molecular regulation of H3K4 trimethylation by Wdr82, a component of human Set1/COMPASS. *Mol Cell Biol*. 2008;28(24):7337–44.
24. Vitaliano-Prunier A, Menant A, Hobeika M, Geli V, Gwizdek C, Dargemont C. Ubiquitylation of the COMPASS component Swd2 links H2B ubiquitylation to H3K4 trimethylation. *Nat Cell Biol*. 2008;10(11):1365–71.
25. Raman SB, Nguyen MH, Zhang Z, Cheng S, Jia HY, Weisner N, Iczkowski K, Clancy CJ. *Candida albicans* SET1 encodes a histone 3 lysine 4 methyltransferase that contributes to the pathogenesis of invasive candidiasis. *Mol Microbiol*. 2006;60(3):697–709.
26. Bolger AM, Lohse M, Usadel B. Trimmomatic: a flexible trimmer for Illumina sequence data. *Bioinformatics*. 2014;30(15):2114–20.
27. Langmead B, Salzberg SL. Fast gapped-read alignment with Bowtie 2. *Nat Methods*. 2012;9(4):357–9.
28. Lerdrup M, Johansen JV, Agrawal-Singh S, Hansen K. An interactive environment for agile analysis and visualization of ChIP-sequencing data. *Nat Struct Mol Biol*. 2016;23(4):349–57.
29. Robinson JT, Thorvaldsdottir H, Winckler W, Guttman M, Lander ES, Getz G, Mesirov JP. Integrative genomics viewer. *Nat Biotechnol*. 2011;29(1):24–6.

## Publisher's Note

Springer Nature remains neutral with regard to jurisdictional claims in published maps and institutional affiliations.